Improved semi-analytical simulation of UT inspections using a ray-based decomposition of the incident fields

Vincent Dorval, Nicolas Leymarie, Sylvain Chatillon

Improved Semi-Analytical Simulation of UT Inspections Using a Ray-Based Decomposition of the Incident Fields

Vincent Dorval[a)], Nicolas Leymarie and Sylvain Chatillon

CEA, LIST, F-91191 Gif-sur-Yvette, France

[a)]*Corresponding author: vincent.dorval@cea.fr*

Abstract. Semi-analytical models are often used for computationally efficient ultrasonic simulations. They typically apply plane-wave or quasi plane-wave approximations to the ultrasonic fields at the location of flaws in order to calculate diffraction coefficients. In favorable cases, the plane-wave approximations used for echo computations in the Civa software yield satisfying results. However, it can lead to inaccuracies in unfavorable cases, such as for wide probe apertures, outside of the focal region, or for beam-splitting or distortion due to irregular geometries. This communication presents an improved model, implemented in a development version of the software. The new approach describes the ultrasonic field as a sum of rays and applies the plane-wave approximation to each ray instead of the entire field. It significantly improves the accuracy of echo computations. However, it implies that the diffraction is calculated for each pair of incident and diffracted rays instead of being calculated only once: a specific algorithm has been developed in order to avoid a significant increase in computation times. Benefits of the new approach are illustrated by comparing its results and computation times to those of the former plane-wave model in several cases of interest. They are also compared to those of a coupled finite element model (Civa-Athena).

INTRODUCTION

The simulation of ultrasonic Non Destructive Evaluation has a wide range of industrial applications. It can, for example, help the design of inspection procedures or the interpretation of measurements. Simulation methods can rely either on semi-analytical methods, numerical methods (such as finite elements), or on a combination of both. Semi-analytical methods apply approximations to perform faster computations than numerical ones, which can come at the cost of a loss of accuracy in their results.

Plane-wave scattering coefficients are used by many semi-analytical methods, including those described by Thompson and Gray [1] and by Schmerr and Song [2], as well as those implemented in the Civa software [3]. Plane-wave and quasi plane-wave approximations of the ultrasonic fields provide the input values for the calculations of these coefficients. The quasi plane-wave approximation allows accounting for some effects of the probe aperture in the spectral content of the echo. This can be done through analytically calculated field coefficients for simple geometries [1]. The Civa approach is meant to be generic and able to handle complex geometries, therefore its field calculations rely on a semi-analytical paraxial ray method. A strict plane wave approximation is applied to these fields during the echo computation and some information is lost about aperture and spectral content. Such an approximation can be more or less accurate, depending on the situation. It typically yields satisfactory results when applied in far field and in the focal axis of the probe, but can produce significant errors when these conditions are not met. The simulation method presented in this communication is being developed with the aim of correcting these errors.

EXPRESSION OF ULTRASONIC ECHOES

Ultrasonic echoes can be expressed using Auld's reciprocity theorem [4]. With some notation modifications and the introduction of the amplitude S_{input} of the input signal, their expression can be adapted into:

$$S_{echo} = S_{input} \int_{\Sigma_F} (\boldsymbol{u}_{Em} \cdot \boldsymbol{T}_{ReF} - \boldsymbol{u}_{ReF} \cdot \boldsymbol{T}\boldsymbol{n}_{Em}) d\Sigma. \quad (1)$$

S_{input} is related to the electric signal that enters the acquisition chain and also accounts for all the filtering effects not related to ultrasonic phenomena. It is considered as an input parameter of the model. $\boldsymbol{u}$ and $\boldsymbol{T}$ refer respectively to the displacement vectors of ultrasonic fields and to their stress tensors projected on the normal of the defect. The indexes *Em* and *ReF* correspond to two configurations: *Em* is the ultrasonic field radiated by the emitting probe when the flaw is absent. *ReF* is the ultrasonic field radiated by the receiving probe when it is acting as an emitter and when the flaw is present. Σ_F is the surface of the flaw. S_{echo}, S_{input} and ultrasonic fields all depend on the frequency.

Expression (1) is general and independent of any approximations. In practice, its evaluation generally requires various degrees of approximation, depending on the approach. In many approaches the expression is approximated in ways that allows replacing the integrand by plane-wave interaction coefficients [1-3]. These coefficients have been obtained analytically for several approximations and types of flaws. Several of them are listed by Schmerr and Song [2].

Based on this, a possible way to compute an echo can be expressed:

$$S_{echo}^{plane\_wave} = S_{input} \sum_{\boldsymbol{x} \in Points} A_{Em}^{\boldsymbol{x}} A_{Re}^{\boldsymbol{x}} C_F^{\boldsymbol{x}} (\boldsymbol{d}_{Em}^{\boldsymbol{x}}, \boldsymbol{p}_{Em}^{\boldsymbol{x}}, \boldsymbol{d}_{Re}^{\boldsymbol{x}}, \boldsymbol{p}_{Re}^{\boldsymbol{x}}) \, \Delta\Sigma. \quad (2)$$

The integral has been replaced by a summation over the surface of the flaw on elements of surface $\Delta\Sigma$ centered around positions $\boldsymbol{x}$. The integrand has been replaced by the product of plane wave amplitudes *A* and of a scattering coefficient C_F. The interaction with the flaw is handled by C_F, the amplitudes *A* of the fields are in the absence of defect. The directions and polarizations **d** and **p** correspond to approximations of the field as plane waves at the location **x**.

In this formalism, the amplitudes *A* also contain phase information concerning the incident and received waves. In the strictest sense of the plane-wave approximation, the phase varies with angular frequency ω *as* $exp(i\omega\tau)$ (or its complex conjugate, depending on conventions), expressing only a time-of-flight τ. In the less quasi plane wave-approximation, the frequency dependence of *A* can account for some effects related to probe aperture.

The semi-analytical echo computation of the Civa software relies on a strict plane-wave approximation, where the waves at a location are described by only their amplitude and time-of-flight. This simplification allows a gain in computation time: both these quantities can be interpolated, which allows doing the costly field computations on a coarse grid, extracting quantities, and then interpolating them on a finer grid. However, it comes at a cost in accuracy.

RAY BASED APPROACH

A decomposition of the field as a sum of rays is readily available in the Civa software, as the ultrasonic field computations of the Civa software rely on them. They can handle complex probe geometry and arbitrary numbers of interfaces with various shapes. To perform echo computations in the plane-wave approximation, the contributions of the rays are summed and the resulting field is approximated. A straightforward way to improve the accuracy of that approach would be to treat each ray as a different plane wave instead of approximating their sum as one. It could be written as follows:

$$S_{echo}^{rays} = S_{input} \sum_{\boldsymbol{x} \in Points} \sum_{i=1}^{N_{Em}^{\boldsymbol{x}}} \sum_{j=1}^{N_{Re}^{\boldsymbol{x}}} A_{ray_{Em}^{i}}^{\boldsymbol{x}} A_{ray_{Re}^{j}}^{\boldsymbol{x}} C_F^{\boldsymbol{x}} \left(\boldsymbol{d}_{ray_{Em}^{i}}^{\boldsymbol{x}}, \boldsymbol{p}_{ray_{Em}^{i}}^{\boldsymbol{x}}, \boldsymbol{d}_{ray_{Re}^{j}}^{\boldsymbol{x}}, \boldsymbol{p}_{ray_{Re}^{j}}^{\boldsymbol{x}} \right) \Delta\Sigma. \quad (3)$$

The sums up to $N_{Em}^{\boldsymbol{x}}$ and $N_{Re}^{\boldsymbol{x}}$ are over the ensembles of rays found between the current point **x** of the defect and the surface of the emitting and receiving probes. This formulations implies that $N_{Em} \cdot N_{Re}$ coefficients C_F need to be computed for each point **x**. This can induce significant increase in computation times compared to equation (2) that only required one coefficient for each point. Keeping computation times low is an important concern here and specific adjustments have been made to this end.

In general, parts of the computation of the interaction coefficient can be performed independently of emission, reception, or both. This allows limiting the operations that are performed $N_{Em} \cdot N_{Re}$ times. Different ways to make the computation faster can be available, depending on the model considered. Examples are given below for the Kirchhoff model for cracks and for an exact model for cylindrical defects. They give a general idea of various ways to perform fast computation. Similar developments have been made for other models, such as the GTD and Born models. Additionally to that, the implementation of the model uses parallel computing over the points **x** of the defect.

Example: the Kirchhoff Approximation for Cracks

The Kirchhoff approximation is also known as the tangent-plane approximation: the field at a point of the surface of a defect is assumed to be equal to the sum of the incident wave and of the waves that would be reflected on a tangent infinite plane. Chapman [5] gives plane-wave coefficients for the entire surface of defects of canonical shapes. It's also possible to perform a discrete sum over the surface, following the forms of equation (2) or (3), in order to deal with defects of any shape. This approach has also the advantage of accounting for variations of the field at the surface, and it is followed by the Civa computation. In the plane-wave approximation, the implementation corresponds to the following equation, whose terms can be identified to those of both (1) and (2):

$$S_{echo}^{plane\_wave} = -S_{input} \sum_{\boldsymbol{x} \in Points} \boldsymbol{u}_{ReF}^{PlaneWaveAndInteraction\_\boldsymbol{x}} \cdot T_{Em}^{PlaneWave\_\boldsymbol{x}} \, \Delta\Sigma. \qquad (4)$$

The term that includes stress in presence of the flaw that appears in (1) vanishes here as the crack is considered as a free surface with no normal stress.

The proposed ray-based version of (4) can be written:

$$S_e^{\,plane\_wave} = -S_{input} \sum_{\boldsymbol{x} \in Points} \left(\sum_{j=1}^{N_{Re}^{\boldsymbol{x}}} \boldsymbol{u}_{ray_{Re}^{j}}^{PlaneWaveAndInteraction\_\boldsymbol{x}} \right) \cdot \left(\sum_{i=1}^{N_{Em}^{\boldsymbol{x}}} T_{ray_{Em}^{i}}^{PlaneWave\_\boldsymbol{x}} \right) \Delta\Sigma. \qquad (5)$$

The brackets around the sums emphasize something important: the emitted and received part can be computed and summed independently from each other. Therefore, the interaction needs only to be computed N_{Re} times, not $N_{Em} \cdot N_{Re}$ times. This can lead to significant gains in computation times.

In the implementation, the results are given the time domain.

Example: Exact Model for Cylindrical Flaws

The problem of the scattering of plane elastic waves by cylinders can be solved exactly for isotropic materials using a separation of variables. For example, Lopez-Sanchez *et al.* [6] give expressions for voids in two dimensions. In Civa, two dimensions versions of the coefficients are implemented for both voids and inclusions. They are used for computations both in two and three dimensions, the latter case being handled by projections and discretization along the axis of the cylindrical defects.

Due to the separation of variable, the scattering coefficient C can be written in the following general form (in the two dimensions case):

$$C(\omega, R, \theta) = \sum_{n=0}^{\infty} F_n(\omega R) G_n(\theta). \qquad (6)$$

In practice, the infinite sum is truncated for calculations. F_n is a function that does not depend on the scattering angle θ and G_n is a function that does not depend on the angular frequency ω or the flaw radius R. For a given echo calculation, the radius and the range of frequencies of interest are constants. Therefore, the required values of F_n can be precomputed. This accelerates significantly the evaluation of equation (3), as the many evaluations of C only require the evaluations of the G_n coefficients and their combination with the corresponding precomputed F_n.

COMPUTATION RESULTS

The ray-based model has been implemented in a development version of the Civa software. Computations were run using three approaches: the existing Civa model based on the plane-wave approximation, the new ray-based

model, and the finite element Civa-Athena hybrid approach [7]. The latter relies on the Athena finite element model for phenomena that occur in a small zone surrounding the defect, while the propagation between the probes and that zone is handled by the same paraxial ray model as the other two models. Finite elements are used here as a reference model for the computation of the interaction between waves and defect. As this approach is only available in 2D, computations with all three models have been performed under 2D assumptions to allow for meaningful comparisons.

The inspected defects are cylindrical in all the cases discussed below, and handled by the exact model described above in the two semi-analytical approaches. This model has the advantage of yielding exact interaction coefficients, which removes one possible source of difference between semi-analytical and finite elements model. It helps isolating the effects of the ray-based description of the fields versus the plane-wave one.

The cylindrical defects are voids with a 2mm diameter. They are located in blocks of steel with longitudinal and transverse wave velocity of respectively 5900 m/s and 3230 m/s, and a density of 7.8 g/cm$_3$. The probes have a diameter of 12.7 mm and a center frequency of 2 MHz.

Comparison of the Results

In the first application case, the defect is located at a depth of 15 mm in the focal axis. The probe moves from a distance of 100 mm to 1 mm of the block. The configuration is illustrated in figure 1(a). The signals obtained by the three methods (not shown here) over all probe positions have similar shapes, but their amplitudes vary and are plotted in figure 1(b).

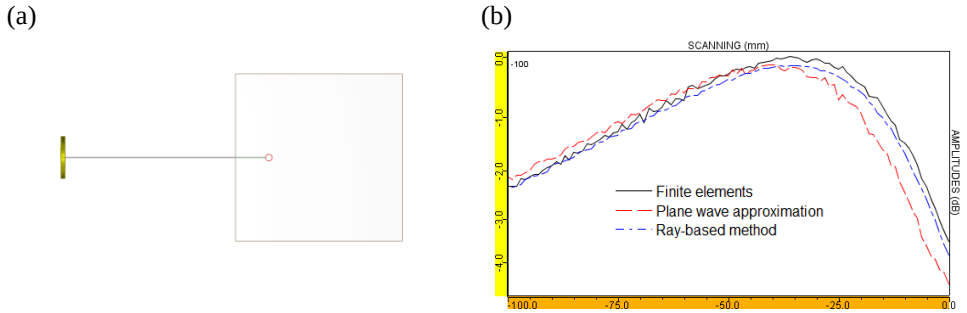

FIGURE 1. (a) Simulated setup for the illustration of near-field effects; (b) Maximum amplitude of the echo from the side-drilled hole as a function of probe distance.

The ray-based method is overall in better agreement with finite elements that the plane wave approximation. The improvement is less than 1 dB in this example but is clearly noticeable on the right side of the plot, which corresponds to short probe-defect distances. A possible explanation for that result is fact that the plane-wave approximation only simulates backscattering in that situation, whereas the ray-based method accounts for the wider range of incident and scattering direction involved. This range is widest when the probe is closest to the defect.

The second case is similar to the first, except that the probe remains at a distance of 10 mm from the block and moves parallel to the surface to a maximum distance of 25mm relative to the vertical of the defect, as illustrated in figure 2(a).

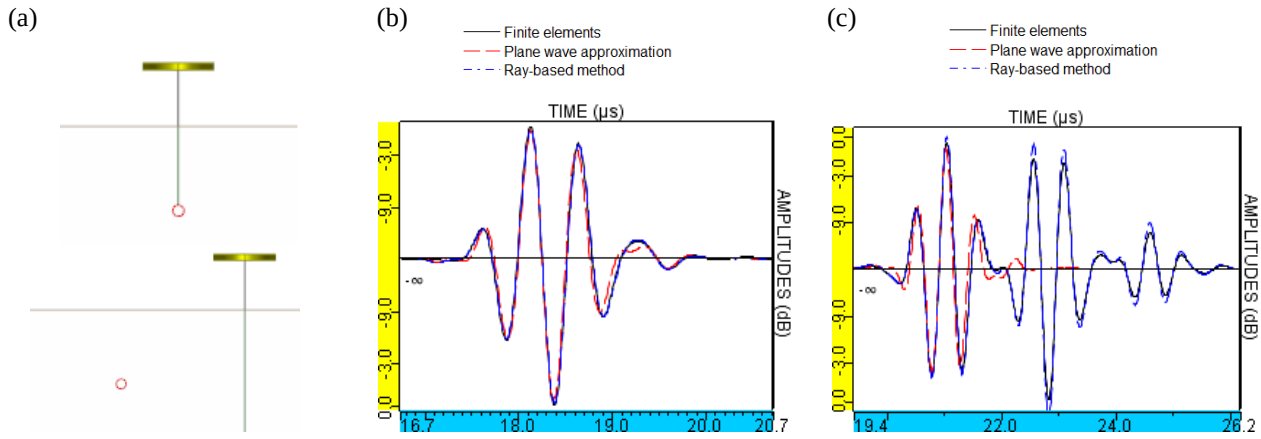

FIGURE 2. (a) Probe positions for the illustration of the effect of probe diffraction; (b) Signals simulated when the probe is above the SDH; (c) Signals simulated when the probe is shifted 25mm away.

Figure 2(b) shows that all three models predict signal echoes of similar shapes when the defect is along the focal axis of the probe, though the plane-wave result is distinguishable from the others and has a slightly lower amplitude (this is more apparent on figure 1(b), where the result at -10 mm correspond to the same probe position as here).

A clear disagreement appears on figure 2(c) where the defect is no longer located along the focal axis. The plane-wave model, which relies on only identifying only a unique plane wave associated with a unique time of flight, is unable to account for the wide range of times-of-flight corresponding to the surface of the probe seen from that angle. To the credit of that model, the maximum amplitude of its signal is not too far from amplitudes of the two others: even in this unfavorable case the plane-wave model can be sufficient if the objective of the calculation is only to have an estimation of the maximum amplitude of the echo. The ray-based model, however, remains in good agreement with finite-elements even for signal shapes thanks to its more complete description of the ultrasonic field.

The next case (figure 3) is a Time Of Flight Diffraction (TOFD) configuration where wedges have been used to emit and receive L waves at a 45 degrees angle. The impact points of the probes are separated by 50 mm and the SDH is at a depth of 15 mm. The results are presented for the L wave echoes at two probe positions.

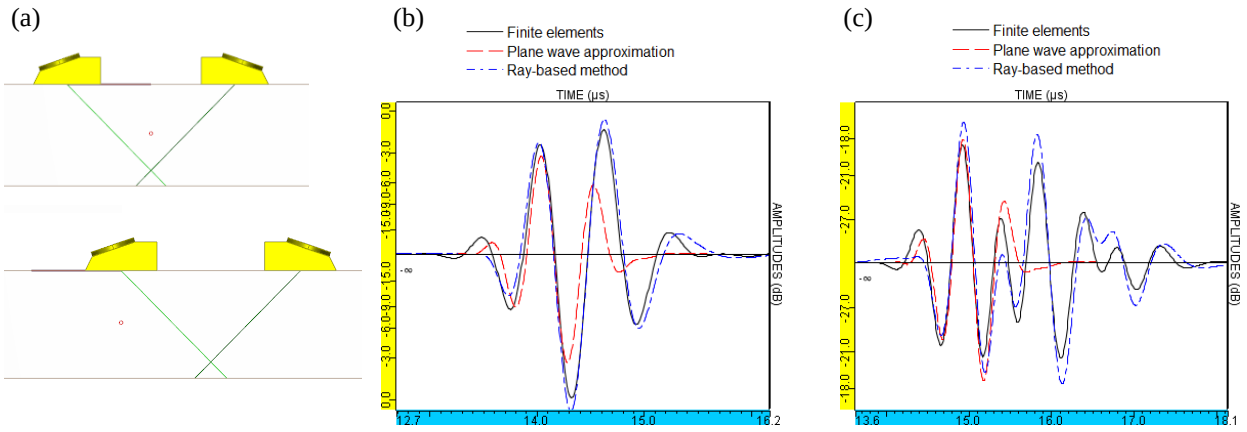

FIGURE 3. (a) Probe positions for the illustration of TOFD simulations out of the focal zone; (b) L-wave signals simulated when probe are positioned symmetrically around the SDH; (c) Signals simulated when one probe is above the SDH.

In this example, the SDH is out of the focal zone for the two probe positions shown. The ray-based method is therefore expected to provide an improvement compared to the plane-wave approximation in both. It appears that this improvement is more significant in figure 3(c), where the signals are more distorted by probe diffraction, than in figure 3(b). As in the previous case, the plane-wave approximation gives a reasonable approximation of the maximum echo amplitudes but the signal shapes are significantly improved by the ray-based method.

In the example illustrated figure 4(a), the surface of the specimen contains a 3mm drop in order to test the ability of the model to take into account the effect of beam-splitting due to a complex geometry. Using the upper section of the surface as a reference, the probe is located 10mm above and the SDH is at a depth of 15mm.

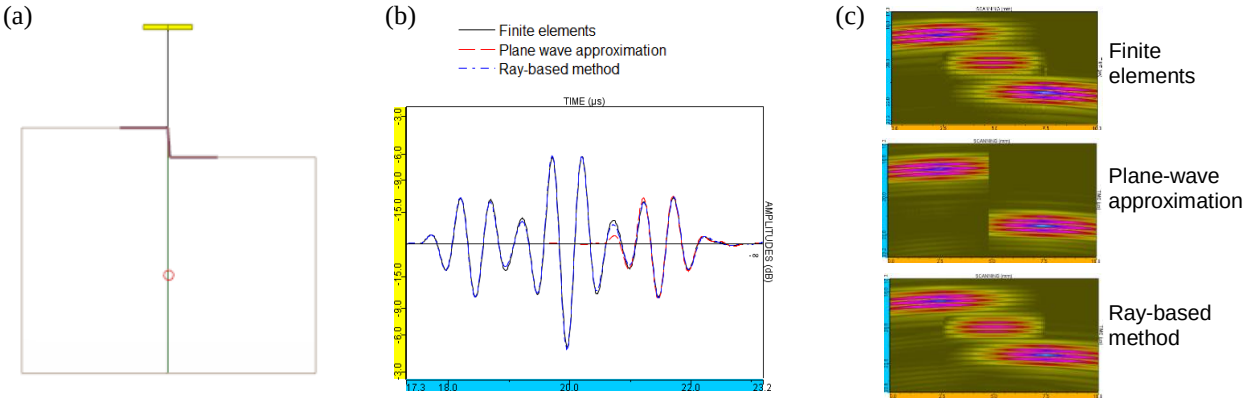

FIGURE 4. (a) Probe positions for the illustration of TOFD simulations out of the focal zone; (b) Signals simulated when the probe is above the SDH; (c) B-scans (time/position representations) for a 10mm horizontal scanning around that position.

The result of figure 4(b) and (c) shows this case is, as expected, very unfavorable to the plane-wave approximation. The ray-based model, on the other hand, manages to match closely finite element results. For all three models, the propagation through the irregular surface is computed by the same ray method: more complex phenomena may occur in reality for this particular case.

No comparisons with experimental results are presented in this communication, but some have been studied in various configurations. Examples are given in [8]. They lead to a similar conclusion as here: the ray-based method tends to be more accurate than the plane-wave approximation.

Computation Times

The previous results show that the new ray-based model allows improving on the plane-wave approximation by being in better agreement with finite elements. However, finite elements are expected to be the most reliable approach of the three in terms of accuracy. The main advantage of semi-analytical methods compared to finite elements, from a user point of view, is their speed. Therefore, the computation times of the new ray-based method have to remain low for it to be viable.

Table 1 summarizes the computation times corresponding to the examples presented in figures 1 to 4. In all of them, the signals have been computed for 101 probe positions.

TABLE 1. Computation times in seconds.

	Example 1	**Example 2**	**Example 3**	**Example 4**
Finite elements	786	1320	508	683
Plane-wave approximation	0.8	0.8	0.9	2
Ray-based method	1.2	4.7	4.4	8.6

For all these configurations, the ray-based method is slower than the plane-wave approximation, but remains several orders of magnitude faster than finite elements.

CONCLUSION

The ray-based method presented here allows overcoming limitations of the plane-wave approximation currently used in the semi-analytical ultrasonic echo computations of the Civa software. Examples of results illustrate some of the situations where the ray-based method is significantly better than the plane-wave approximation, due to the

position of the defect relative to the focal zone or to the part geometry. The most noticeable improvement is the shape of the signals. The maximum amplitudes are also generally more accurate with the ray-based model.

The improvement due to the new method comes at a cost in computation times, though that cost has been limited through optimization and parallelization. Ongoing work aims at further reducing computation times and at making the ray-based method available in a future release of Civa.

REFERENCES

1. R. B. Thompson and T. A. Gray, J. Acoust. Soc. Am. **74** (4), 1279-1290 (1983).
2. L. W. Schmerr and J. S. Song, "Ultrasonic Measurement Models" in *Ultrasonic Nondestructive Evaluation Systems: Models and Measurements* (Springer, New York, 2007), pp. 301-322.
3. M. Darmon, N. Leymarie, S. Chatillon and S. Mahaut, "Modelling of scattering of ultrasounds by flaws for NDT" in *Ultrasonic Wave Propagation in Non Homogeneous Media*, edited by A. Leger and M. Deschamps (Springer, Berlin, 2009), pp. 61-71.
4. B. A. Auld, Wave Motion **1**, 3-10 (1979).
5. R. K. Chapman, "Ultrasonic scattering from smooth flat cracks: an elastodynamic Kirchhoff diffraction theory," Central Electricity Generating Board report NWR/SSD/84/0059/R (1984).
6. A. L. Lopez-Sanchez, H. J. Kim, L. W. Schmerr and A. Sedov, J. Nondestruct. Eval. **24** (3), 83-96 (2005).
7. S. Mahaut, N. Leymarie, A. S. Bonnet-Ben Dhia, P. Joly, F. Collino, T. Fouquet, C. Rose, O. Dupond and F. Foucher, "Simulation of complex ultrasonic NDT cases using coupled analytical-numerical method : the Mohycan Project" in *Proceedings of the 10th European Conference of NDT*, Moscow, 2010, pp. 3621-3628.
8. G. Toullelan, R. Raillon, S. Chatillon, V. Dorval and S. Lonne, "Results of the 2015 UT Modeling Benchmark Obtained with Models Implemented in CIVA" in these proceedings.